Performance Comparison of Different Desiccant Material Based Wheels for Air Conditioning Application

Yadav, Laxmikant
Department of Mechanical Engineering, National Institute of Technology

Ashutosh Kumar Verma
Department of Mechanical Engineering, National Institute of Technology

Dabra, Vishal
Department of Mechanical Engineering, PIET

Yadav, Avadhesh
Department of Mechanical Engineering, HBTU

https://doi.org/10.5109/6792886

出版情報：Evergreen. 10 (2), pp.912-923, 2023-06. 九州大学グリーンテクノロジー研究教育センター
バージョン：

Performance Comparison of Different Desiccant Material Based Wheels for Air Conditioning Application

Laxmikant Yadav[1], Ashutosh Kumar Verma[1], Vishal Dabra[2,*], Avadhesh Yadav[3]

[1]Department of Mechanical Engineering, National Institute of Technology, Hamirpur, HP, India

[2]Department of Mechanical Engineering, PIET, Haryana, India

[3]Department of Mechanical Engineering, HBTU, Kanpur, UP, India

*Author to whom correspondence should be addressed:

E-mail: vishaldabra1987@gmail.com

(Received February 23, 2023; Revised May 24, 2023; accepted June 6, 2023).

Abstract: The purpose of this study is to compare different desiccant materials based desiccant wheel for air conditioning applications using a mathematical model. Seven desiccant material wheels are categorized into three groups. The results revealed that the desiccant wheel made of group 2 materials has a higher temperature-difference in comparison to other groups. So, these desiccant wheels cannot be recommended for air-conditioning applications. For higher ranges of process inlet temperature (40 to 50℃), moisture removal obtained from group 2 wheels is higher than the other wheels and also obtains approximately similar ΔT. But in lower ranges of process inlet temperature (10 to 20℃), group 3 wheels give higher MR with moderate ΔT. although the temperature difference is higher but, due to the higher moisture removal, group 3 wheels can be the preferable choice.

Keywords: Desiccant wheel Materials; Mathematical model; rotary dehumidifier; Solid desiccant.

1. Introduction

In air conditioning systems, controlled temperature (T) and relative humidity (RH) of the supply air play a key role in getting comfort conditions. Desiccant wheel-based air conditioning systems (DWBACS) perform the same role to maintain the Temperature (T) and Relative humidity (RH) of the supply air[1–3]. Desiccant wheel regeneration is possible with solar heat or waste heat. Flat plate heat collector[4] and Parabolic dish collector can also be utilized to collect solar heat[5]. For process air, it was observed that the RH of air decreases with an increase in temperature 'T'. The increase in 'T' of the process air increases the sensible load of the cooling unit of DWBACS and decreases the performance of DWBACS[6,7]. In literature, many researchers discussed the causes of an increase in the temperature difference (ΔT) of process air of the desiccant wheel and identified that carry-over heat and heat of adsorption are the two main parameters that affect the temperature of the process air. Carry-over heat is associated with the rotating matrix when it comes from the hot region (hot air flow region) to the colder region (process airflow region). This heat originates from the hot regeneration air, and if higher regeneration (reactivation) temperature is maintained, then it increases the ΔT. But this can be controlled by decreasing the temperature of the air heater. The regeneration temperature required for the regeneration of the dehumidifier depends upon the type of adsorbent used in the wheel. The heat of adsorption is the second cause of an increase in ΔT[8]. The heat of adsorption is the heat which releases when moisture transfer takes place from air to desiccant due to vapour pressure difference. The transferred moisture is adsorbed on the surface and forms a single or multi-layer depending upon the isotherms. After that, adsorbed vapour enters into the micro-pores of the desiccant, and due to capillary action, condensation occurs and releases heat[9]. But, the heat of sorption is slightly more than the latent heat of condensation of water because the heat of sorption is the summation of the heat of wetting and latent heat[10]. The heat of wetting on the desiccant surface varies with the saturation vapour pressure level of the adsorbent. Hence, we can say that the heat of adsorption will be more when more moisture is adsorbed on the desiccant[11]. Conclusively, moisture removal (MR) and exit temperature of process air depend upon the specific surface area and pore diameter of the desiccant[12] because it affects the capillary action and capillary action directly affects the heat of adsorption[13].

A lot of work has been conducted by several researchers on reactivation temperature and carry-over heat. Researchers[14–17] studied the influence of

reactivation temperature on the dehumidification ability of the dehumidifier. They observed that the higher reactivation temperature is not desirable as it decreases the DCOP of the dehumidifier and increases the exit temperature of process air[18]. Silica gel and zeolite are the widely accepted desiccant wheel for use in the solid desiccant cooling system[19]. and these solid desiccants can be regenerated in the temperature ranges of 60 to 120°C[20]. In higher reactivation temperature, the dried air temperature of the rotary dehumidifier is relatively higher than the lower reactivation temperature case due to carry-over heat. This problem can be reduced by searching low regeneration temperature desiccant wheel. Alternative low regeneration temperature desiccant materials have been used in the desiccant wheel in reference[21]. In this work, they compared the two desiccant wheel material super-adsorbent polymer and Zeolite (FAM-Z01 of 7.3 Å pore size) with existing silica gel rotary dehumidifier, and they found that in lower regeneration temperatures and humid environment, the super-adsorbent polymer rotary dehumidifier performs better than the silica gel desiccant wheel. In Research[22] Polymer sorbent, activated carbon-based adsorbents, and silica gel water vapour absorption behavior were compared. Further, to reduce the effect of carry-over heat, the purge section was introduced by researchers[23–25], and they reported that the purge section not only controls the (ΔT) but also reduces the consumption of regeneration energy.

In order to lower the ΔT of the rotary dehumidifier, several new designs of desiccant wheels were introduced by the researchers[26]. The idea of a diabatic rotary dehumidifier was introduced[6]. Similarly, Researchers[7] invented the novel design of the desiccant wheel heat exchanger to lower ΔT, like a desiccant-coated heat exchanger (DCHE).

This work is primarily related to the type of desiccant used in the rotary dehumidifier. Hence, it is necessary to introduce the characteristics of the different desiccant materials which have been studied in the literature. Numerous investigators mathematically and experimentally studied the various aspects of the different desiccant materials over the year. Heat and moisture transfer process of a composite rotary dehumidifier made of inert and desiccant material and investigated the moisture removal effectiveness of the adsorption and regeneration process[27]. The moisture removal ability of silica gel and composite desiccant (silica gel–$CaCl_2$) was compared[28], and they found that the hygroscopic capacity of the composite desiccant was much higher than the silica gel desiccant wheel. Performance of a novel silica gel haloid compound desiccant wheel at different operating conditions predicted[16], and they found better performance in humid weather. Experiments were performed to assess the performance of a new zeolite rotary dehumidifier, which could have been regenerated at low regeneration temperature[29]. Experimentally and numerically studied the dehumidification effectiveness of new zeolite rotary dehumidifiers at a wide range of wheel inlet conditions[30]. Performance of 10 types of desiccant beds with different reactivation temperatures for different environmental conditions based on specific dehumidification power (SDP), COP, and dehumidification efficiency (DE) studied[31]. But the comparison of these desiccants for rotary dehumidifiers under other operating conditions (in addition to regeneration temperature) like rotational speed, regeneration, and process velocity has not been investigated yet. Furthermore, a comparison of various desiccant wheels to analyze the 'ΔT' of process air has not also been investigated yet. Therefore, in this paper, seven different desiccant material namely, Silica gel-A, Silica gel-B, Silica gel-RD, $CaCl_2$, LiCl, Composite silica gel-LiCl, and Composite silica gel-$CaCl_2$, based wheels' performance has been compared by analyzing the 'MR' and 'ΔT' of process air. Further, these materials also require a higher reactivation temperature to regenerate which results in a higher ΔT of these wheels compared to other desiccant wheels. Desiccant material economics go beyond their initial cost. Desiccant-based systems are economically viable due to regeneration, reusability, operational lifetime, energy consumption, and system efficiency. Some economic details of above selected desiccant materials are discussed in table 1.

Table 1: Economic details of selected desiccant materials

Silica gel-A, B, and RD	Silica gel is a popular desiccant due to its effectiveness and affordability. It's inexpensive. Silica gel is widely available and cheaper to produce than other desiccants
Calcium Chloride	It costs more than Silica gel. CaCl2 desiccants cost differently depending on purity and grade. They have a higher moisture absorption capacity than Silica gel, which can extend operating lifetimes and offset the higher initial cost.
Lithium chloride	Lithium chloride is another desiccant with high moisture absorption properties. However, LiCl desiccants tend to be more expensive than Silica gel due to the higher cost of lithium chloride as a raw material.
Composite silica gel-LiCl and Composite silica gel-CaCl2	They combine the moisture absorption of silica gel with the enhanced performance of the added desiccant material. The composition and manufacturing process of composite desiccants affect their economics. Due to processing and materials, composite desiccants cost more than individual desiccant materials.

2. Mathematical model

One-dimensional numerical model can be used for the modeling of the rotary dehumidifier because the thickness of the desiccant coated on the substrate is very thin i.e., order of 0.2 mm[32]. Further, a one-dimensional numerical model is easy to solve and also reduces computational time. The frontal cross-section of the rotary dehumidifier is shown in Fig. 1, which indicates that it has many uniform sinusoidal channels. The schematic diagram of one sinusoidal channel is shown in

Fig. 2(a) and 2(b), which indicates the substrate, desiccant layer, and dimensions of the channel.

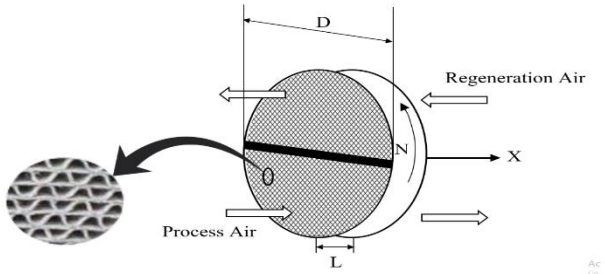

Fig. 1: Rotary desiccant wheel showing cross-section with many sinusoidal channels

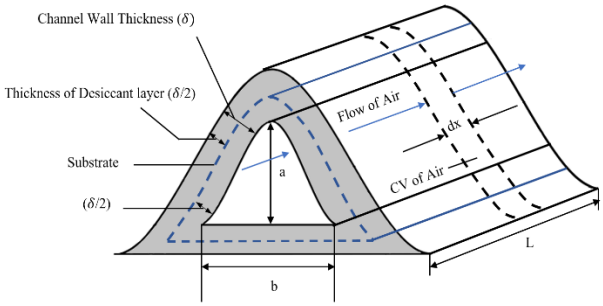

Fig. 2 (a): Sinusoidal channel indicating substrate, desiccant layer, and channel dimensions[12)]

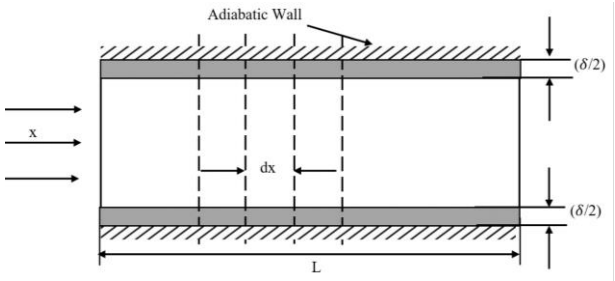

Fig. 2 (b): Differential control volume of air and desiccant wall of the sinusoidal channel[12)]

Out of these channels, only one sinusoidal channel of length dx has been considered as differential control volume, as shown in Fig. 2(a) and fig. 2(b) for the derivation of heat and mass transfer equations.

2.1 Assumptions followed for the derivation of the equations

The following assumptions have been considered for the derivation of governing equation:

1. The rotary desiccant wheel is divided into equal process and regeneration sectors. The desiccant wall is made of substrate material (glass fiber) and a desiccant layer as shown in Fig. 2(a). This wall is shared by two channels.
2. The mathematical model is one-dimensional (axial) and transient.
3. Solid side resistance, like conduction resistance and mass diffusion, have been neglected in moist air. Similarly, the diffusion of water vapour in the axial direction of the desiccant wall has been neglected.
4. It has been assumed that there is no leakage of air streams from the different regions.
5. The inlet conditions of the moist air have been assumed to be uniform.
6. It has been assumed that the coefficient of heat and mass transfer between the desiccant wall and moist air is constant throughout the flow channel. Similarly, the thermophysical properties of moist air, desiccant, and substrate have also been kept constant.
7. Due to low rotational speed, the centrifugal effect has been neglected.

2.2 Heat and Mass Transfer Equations

The differential control volume (CV) of Fig. 2(a) and 2(b) is split into two parts i.e., CV of moist air and CV of the desiccant wall. The mass and energy conservation have been applied on the CV of the air and desiccant layer and derived two mass and two energy equations based on the above assumptions. These equations are presented below:

Final mass conservation equation derived from the CV of moist air:

$$\left[\frac{\partial Y_a}{\partial t} + u\frac{\partial Y_a}{\partial x}\right] = \left[\frac{h_m P_f (Y_d - Y_a)}{\rho_{da} A_{csf}}\right] \qquad (1)$$

Final mass conservation equation derived from the CV of the desiccant layer:

$$\left[\epsilon\rho_{da}\frac{\partial Y_d}{\partial t} + \varphi\rho_{ad}\frac{\partial W}{\partial t}\right] = \left[\frac{h_m P_f (Y_a - Y_d)}{A_{csdl}}\right] \qquad (2)$$

Final energy conservation equation derived from the CV of moist air:

$$\frac{1}{P_f}\left[\frac{\partial T_a}{\partial t} + u\frac{\partial T_a}{\partial x}\right] = \left[\frac{h(T_d - T_a) - h_m(Y_a - Y_d)c_{pv}(T_a - T_d)}{\rho_{da}(c_{pda} + Y_a c_{pv})(A_{csf})}\right] \qquad (3)$$

Final energy conservation equation derived from the CV the desiccant layer:

$$\left[\{\varphi\rho_{ad} - (\varphi+1)\rho_m\}\{\varphi c_{pad} - (\varphi+1)c_{pm}\} + \varphi\rho_{ad}c_{pw}W\right]\frac{\partial T_d}{\partial t} + \varphi\rho_{ad}c_{pw}T_d\frac{\partial W}{\partial t} - k_d\frac{\partial^2 T_d}{\partial x^2} = \left[\frac{P_f\{h(T_a - T_d) + h_m(Y_d - Y_a)c_{pv}(T_d - T_a) - h_m(Y_d - Y_a)q_{ads}\}}{A_{csdl}}\right] \qquad (4)$$

The above four one-dimensional equations contain five unknown variables. The variables are Y_a, Y_d, W, T_a, T_d. In order to solve equations (1) to (4), some initial & boundary conditions, the equation of isotherm, and other auxiliary equations are also required that are discussed in sections 2.3 and 2.4.

2.3 Boundary Conditions for Two-Sector Rotary Dehumidifier

The following boundary conditions will be applicable for the above heat and mass transfer equations:

For the process (adsorption) sector

$T_{air}(0,t) = T_{process,in}$

$Y_{air}(0,t) = Y_{process,in}$

For the regeneration sector

$T_a(L,t) = T_{regeneration,in}$

$Y_a(L,t) = Y_{regeneration,in}$

Initial Conditions for Two-Sector Rotary Dehumidifier

$T_{air}(x,0) = T_{a0}$

$T_{desiccant}(x,0) = T_{d0}$

$Y_{air}(x,0) = Y_{a0}$

$Y_{desiccant}(x,0) = Y_{d0}$

$W(x,0) = W_0$

2.4 Auxiliary Equations

The relation between specific humidity Y_d, and relative humidity RH can be expressed as:

$$Y_d = \frac{0.62188P_v}{P_a - P_v} = \frac{0.62188RH_d}{\frac{P_a}{P_{vs}} - RH_d} \quad (5)$$

The saturation pressure p_{vs} of equation 5 is the function of temperature, and it can be related according to reference[33]:

$$P_{vs} = e^{\left(23.196 - \frac{3816.44}{T_d - 46.13}\right)} \quad (6)$$

To relate W and RH, the below sorption isotherm equation is used expressed in reference[34]:

$$RH_d = \frac{R \times \frac{W}{W_{max}}}{1 + (R-1) \times \frac{W}{W_{max}}} \quad (7)$$

Equation (7) is a very important auxiliary equation. It contains term RH_d, R, W and W_{max}. The term R is called the separation factor; it determines the nature of the isotherm shape. The value of R and W_{max} for different desiccants is given in reference[31]. Similarly, the heat of adsorption (h_{ads})for different desiccant materials is also given in reference[31], also tabulated in the result discussion section.

Nusselt number can be expressed according to reference[26]

$$Nu = \frac{(Nu_t + Nu_h)}{2} \quad (8)$$

$$Nu_t = 1.1791\left[1 + 2.7701\left(\frac{a}{b}\right) - 3.1901\left(\frac{a}{b}\right)^2 - 1.9975\left(\frac{a}{b}\right)^3 - 0.4966\left(\frac{a}{b}\right)^4\right] \quad (9)$$

$$Nu_h = 1.903\left[1 + 0.455\left(\frac{a}{b}\right) + 1.2111\left(\frac{a}{b}\right)^2 - 1.6805\left(\frac{a}{b}\right)^3 + 0.7724\left(\frac{a}{b}\right)^4 - 0.1228\left(\frac{a}{b}\right)^5\right] \quad (10)$$

Since heat and mass transfer occur simultaneously between air and desiccant, so Sherwood number is also required to relate with the Nusselt number. The formula of Sherwood Number is:

$$Sh = \frac{h_m D_{hf}}{D_m} \quad (11)$$

In order to relate the heat transfer coefficient with the mass transfer coefficient, the Colban Chilton analogy is used, and according to this analogy Sherwood Number and Nusselt number are related as:

$$Sh = Nu \times Le^{1/3} \quad (12)$$

The Lewis number (Le) is equal to 1 for the water vapour air mixture

$$Sh = Nu$$

$$\frac{h_m D_{hf}}{D_m} = \frac{hD_{hf}}{k}$$

$$h_m = \frac{hD_m}{k} \quad (13)$$

The coefficient of diffusion of water vapour in the air can be expressed according to the reference[33]:

$$D_m = \frac{2.302}{10^5} \times \frac{P_0}{P_{atm}} \times \left(\frac{T}{T_0}\right)^{1.81} \quad (14)$$

Where, $P_0 = 98000$ Pa, and $T_0 = 256$ K

2.5 Method of Solution

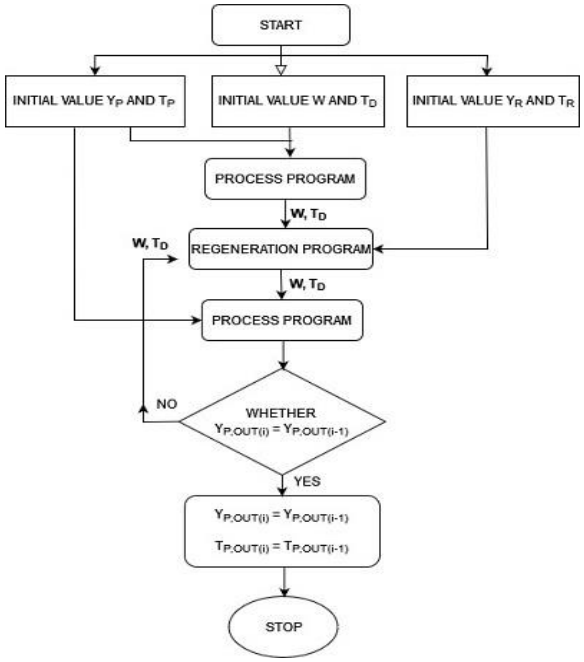

Fig. 3: Program flow chart of two-sector rotary dehumidifier

The governing equations of sections 2.2 and 2.4 have been solved with the help of partial differential equation solver software named "FLEXPDE" with appropriate boundary conditions. In this study, the rotary dehumidifier has been divided into equal process and regeneration sectors. So, two programs code have been prepared for the process and regeneration sector in the script of the software FlexPDE. These programs are linked to each other as governing equations are linked. The Program flow of the chart of FlexPDE for two-sector rotary dehumidifiers is given in fig. 3.

3. Validation of mathematical model with experimental results

The developed model has been solved by FlexPDE software, and the results found from the FlexPDE have been validated with the experimental results conducted in the research[35]. In research[35] $Y_{p,\ out}/Y_{p,\ in}$ has been experimentally analyzed at different rotational speeds, and variation is plotted, which is shown in Fig. 4. In order to conduct the experiments, the following operating conditions and desiccant wheel specifications were used, which are shown in Table 2.

In order to analyze $Y_{p,\ out}/Y_{p,\ in}$ at different rotational speeds, the same input conditions of Table 2 have been entered in the script of FlexPDE, and results are plotted and merged in Fig. 4 for comparison. It is observed that the same trend of the curve has been obtained for both the simulation and experimental results. The maximum deviation of mathematical (simulation) results from the experimental data[35] is less than 10% in the specified ranges of the speed of Fig. 4. So, it is a good agreement between simulation results and experimental values. An optimal rotational speed of the dehumidifier is required for minimum exit humidity ratio, but this optimal speed is different for each condition of the experimental and numerical results.

Table 2: Operating conditions and wheel specification used for conducting experiments[35]

No. of EXP	Inlet humidity ratio (kg kg^{-1})	Inlet process temperature (°C)	Inlet Regeneration temperature (°C)	DW specifications for conducting the experiments
EXP I	0.009	25	80	L=0.2 m b=0.0032 m a=0.0018 m δ_d=0.0002 m Process area /Regeneration area=3.3
EXP III	0.00805	25	160	
Process and regeneration inlet velocity= 1m/s				

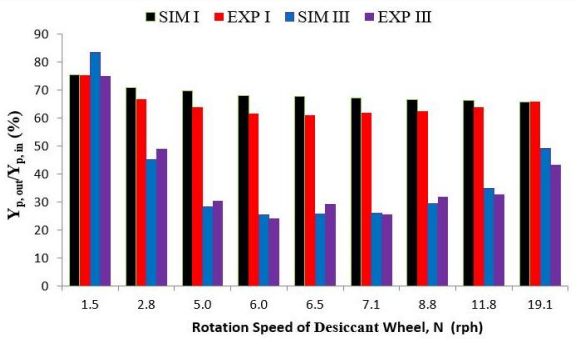

Fig. 4: Comparative plot of $Y_{p,\ out}/Y_{p,\ in}$ vs N for simulation and experimental results according to Table 2

4. Results and discussion

In this analysis, seven different desiccant wheels(materials) have been compared based on moisture removal and ΔT andcategorized into three groups due to their similar nature. Group 1 includes three types of silica gel, i.e. silica gel B, silica gel 3A, and silica gel RD while group 2 includes Calcium Chloride ($CaCl_2$) and Lithium Chloride (LiCl). Group 3 considers two composite desiccants, which are silica gel- lithium chloride and silica gel- calcium chloride. The term MR and ΔT are the two performance indices of the desiccant wheel, which are plotted at different operating conditions in section 4.1. The term MR can be defined as, $MR = Y_{p,in} - Y_{p,out}$. Similarly, ΔT can be defined as, $\Delta T = T_{p,in} - T_{p,out}$.

Table 3: Different thermo-physical properties of solid desiccant materials[31]

	Desiccants	c_{pad} (kJ/ kg-K)	k_d (W/ m-K)	ρ_{ad} (kg/ m^3)	W_{max} (kg/ kg)	q_{ads} (kJ/ kg)	ε
Group 1	Silica gel B	0.921	0.198	790	0.4	2362	0.5
	Silica gel 3A	0.921	0.174	770	0.35	2380	0.56
	Silica gel RD	0.921	0.198	800	0.37	2370	0.44
Group 2	$CaCl_2$	0.620	0.21	2150	0.33	3675	0.01
	LiCl	1.132	0.65	2068	0.43	2957	0.08
Group 3	Silica gel/ LiCl	0.924	0.239	875	0.6	2476	0.36
	Silica gel/ $CaCl_2$	0.866	0.32	976	0.55	2620	0.41

Various properties of desiccants are given in Table 3. Physical structures of Group 1 material are given in Table 4 to explain the adsorption phenomenon based on surface area and pore size. Since the adsorption capacity of any desiccant material depends upon the type of isotherm. Silica gel RD is in the category of type-I isotherm because it performs better at lower RH due to higher specific surface area and less pore size. Contrarily, silica gel B is in the category of isotherms which have higher adsorption capacity at higher RH because of its lower specific surface area and larger pore diameter as explained in the research[13].

Table 4: Physical structures of group 1 material[31)]

Type of Silica Gel	Surface Area per gram (m^2/g)	Volume of porous (ml/g)	Average Diameter of pore (nm)
Silica gel B	476	0.61	4.78
Silica gel 3A	606	0.45	3.0
Silica gel RD	650	0.35	2.1

Table 5: Specifications of the rotary dehumidifier

Rotary dehumidifier length, L(cm)	2
Diameter of the desiccant wheel, D(cm)	37
Ratio of process area to regeneration area	1:1
Thickness of the sinusoidal channel wall, δ(mm)	0.2
Pitch of flow passage of sinusoidal channel, b(mm)	3.2
Height of flow passage of sinusoidal channel, a(mm)	1.8
Volume ratio of desiccant, (φ)	0.7

Further, to solve one-dimensional heat and mass transfer equations using FlexPDE following the specification of the desiccant wheel is required which is given in Table 5, and these specifications of the rotary dehumidifier have been used for finding the results at different operating conditions which are given in Table 6 and discussed in section 4.1.

Table 6: Variation of operating parameters and fixed value used for the analysis

Name of Operating Parameters	**Parametric variations**	**Fixed value**
Process inlet air temperature (℃)	15-50	30
Process inlet specific humidity ($kg\ kg^{-1}$)	0.005-0.035	0.024
At 30℃ DBT and 0.024 kg of water vapour/kg of dry air, the value of RH in %	-	90%
Inlet regeneration air temperature (℃)	60-160	60
Rotational speed of the wheel (rph)	5-40	10
Process air inlet velocity ($m\ s^{-1}$)	1-6	4
Regeneration air inlet velocity ($m\ s^{-1}$)	1-6	2

4.1 Analysis of Different Desiccant Wheels at Different Operating Conditions

4.1.1 Analysis of the MR and ΔT of process air at a different rotational speed of the wheels

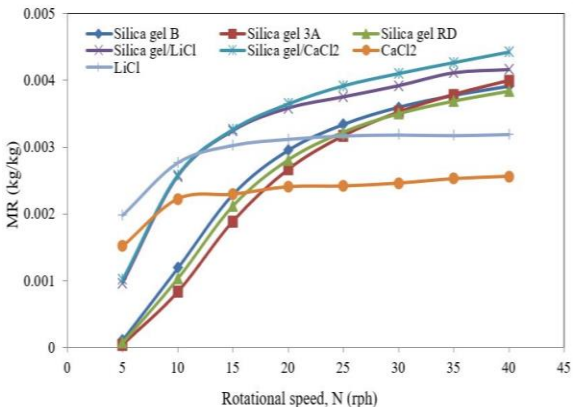

Fig. 5: Graph of MR with N for different desiccants wheels

Fig. 5 shows the comparison of different desiccant wheels with rotational speed (N), and it is observed that in between 15 to 40 rph, group 3 wheels have higher moisture removal than the other wheels because Group 3 materials are Composite of silica gel-LiCl and Composite of silica gel-CaCl2. Added materials (LiCl and CaCl2) enhaunce the moisture absorption property of silica gel. The trend of MR is almost similar for group 1 wheels and it is observed that silica gel B yields slightly higher MR compared to other materials of group 1 because the wheel is operating at a higher RH (90%) as per Table 6. At higher RH silica gel B performs better due to its desirable physical structure presented in Table 4. The nature of silica gel B of group 1 is a similar trend in further cases also. There is a significant effect of speed on group 3 from 5 to 20 rph, after this rise in moisture removal decreases and the curve becomes flat. However, for group 1 wheels, the curve starts flattening at a higher speed compared to group 3. Because the heat of adsorption of group 3 is higher than group 1 and the higher speed (beyond 20 rph) is too fast to remove the desiccant heat properly. Due to this, the vapour pressure difference starts decreasing and the curve starts flattening. This trend has been also concluded in the research[36)].

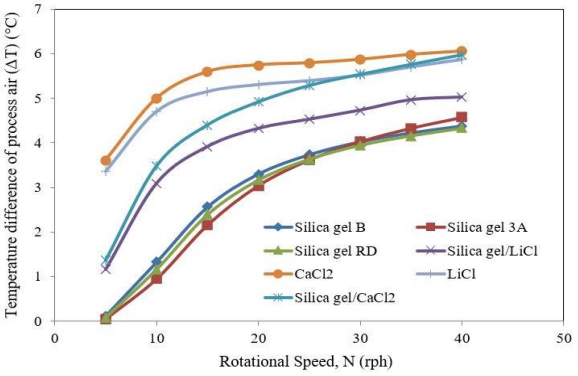

Fig. 6: Graph of temperature difference with N for different desiccant wheels

There is less effect of rotational speed on group 2 material, because, after 15 rph, MR is almost constant. Because the heat of adsorption of group 2 wheels is large which heats the desiccant surface, and due to this equilibrium is reached between air and desiccant surface. Further, a speed beyond 15 rph may be too fast to remove the heat of the desiccant properly. If we compare all three groups, then it can be observed that in the lower range of speeds group 2 and group 3 are better wheel choices. But overall group 3 is more suitable for better moisture removal.

Fig. 6 shows that of nature of the curve for temperature difference is similar to the MR. Here group 2 wheels have a larger temperature difference among all desiccants due to the larger heat of adsorption. Since the regeneration temperature is the same (60 ℃) for all materials, so almost the same heat is transferred to the dehumidification zone from the regeneration zone. Also, a lower value of thermal conductivity and specific heat is not in favor of carry-over heat. Hence, only the heat of adsorption plays a dominant role to increase the temperature of dehumidified air and this explanation is also applicable to further results of ΔT. The MR of group 2 is lower than group 3 in most of the rotational speeds. As we know, an increase in temperature difference unnecessarily increases the cooling load of DWBACS. For less temperature difference, group 1 will be a suitable wheel, but the MR of this type of wheel is low. Therefore, for higher MR and moderate temperature differences, group 3 can be selected as the better wheel.

4.1.2 Analysis of MR and ΔT of process streams at different regeneration stream velocity

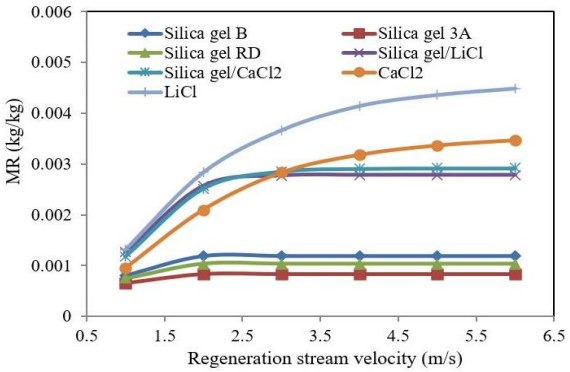

Fig. 7: Graph of MR with regeneration stream velocity for different desiccant wheels

Fig. 7 shows the comparison of different desiccants with regeneration stream velocity, and it can be observed that 2 m/s is the optimum value of the regeneration stream velocity for group 1 and 3 wheels. While the optimal regeneration stream velocity for group 2 wheels lies on the higher regeneration velocities. A higher regeneration energy is required to remove the condensed vapour from the desiccant pores because it includes latent heat of vaporization also and the group 2 materials have higher condensed vapour due to higher heat of adsorption. Therefore, in the ranges of higher regeneration stream velocity, proper regeneration takes place and that increases the MR. However, higher regeneration stream velocity is not desirable because it increases the pumping power of the fan. Although the MR of group 2 is more in the ranges of higher velocity, Even then group 3, is preferable because of moderate MR and less pumping power than group 2 wheels.

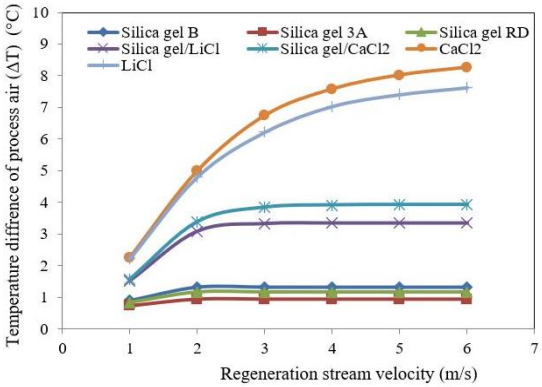

Fig. 8: Graph of temperature difference with regeneration stream velocity for different desiccant wheels

A similar trend of the curve is also obtained for temperature difference which is shown in Fig. 8. But from Fig. 8 it can be observed that the temperature difference of process air for group 2 is more than the other desiccants due to the larger heat of adsorption which is not desirable. Therefore, it can be concluded that group 3 material is the best choice for the selection of the desiccant for the rotary dehumidifier. Further, Fig. 7 and Fig. 8 indicate that $CaCl_2$ has a relatively lower moisture removal than LiCl but the temperature difference of $CaCl_2$ is relatively higher than LiCl due to more heat of adsorption.

4.1.3 Analysis of the MR and ΔT of process air at different regeneration air temperature

Similar to the previous case, here also there is very less influence of regeneration air temperature on group 1 wheels. Fig. 9 shows that the MR of group 1 slightly increased from 50 to 60℃ and then becomes constant. But for group 2, MR increased up to the endpoint, i.e., 120℃. The reason for this has been already discussed in the previous case. If we have a higher regeneration temperature, then we may go for the selection of group 2 but it also increases the regeneration energy of the wheel thus it may decrease the DOCP of the dehumidifier. For group 3, MR increases from 50 to 80℃ and then becomes steady. Further, its MR is slightly higher than $CaCl_2$ but slightly lower than LiCl. But its suitability to lower regeneration temperature without compromise in MR, recommends group 3 as the better choice.

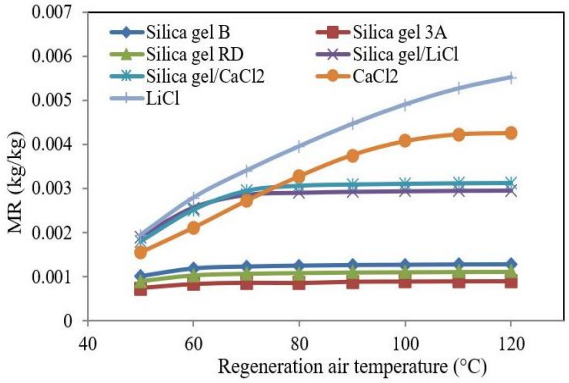

Fig. 9: Graph of MR with regeneration air temperature for different desiccant wheels

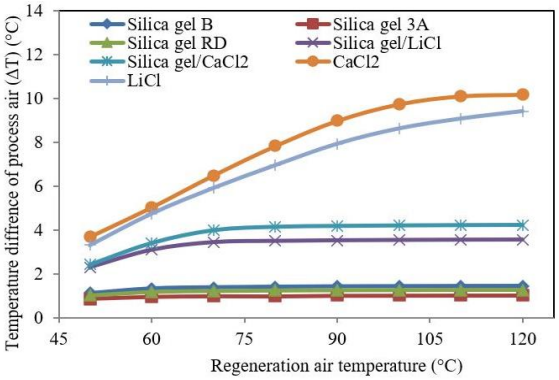

Fig. 10: Graph of temperature difference with regeneration air temperature for different desiccant wheels

Fig. 10 shows that there is very little influence of regeneration air temperature on a temperature difference of group 1 wheels, and a moderate effect on group 3 i.e. up to 50 to 70℃, but a significant effect on group 2 wheels. Therefore, group 2 materials can be considered temperature-sensitive materials, especially $CaCl_2$ due to their larger heat of sorption. In this case, also group 3 materials can be considered better desiccants because MR is higher in lower regeneration temperature ranges which increases the overall COP of the system. Another benefit is that increase in temperature difference is also less than group 2 which will reduce the cooling load of the DWBACS system.

4.1.4 Analysis of the MR and ΔT of process air at different process stream velocity

As it is well-known fact that a rise in process stream velocity reduces moisture removal due to less residence time. Fig. 11 shows that MR is higher for group 2 wheels and the effect of process velocity is also greater on group 2 wheels compared to groups 3 and 1. Because the higher velocity of the process section properly removes the heat of adsorption of the desiccant.

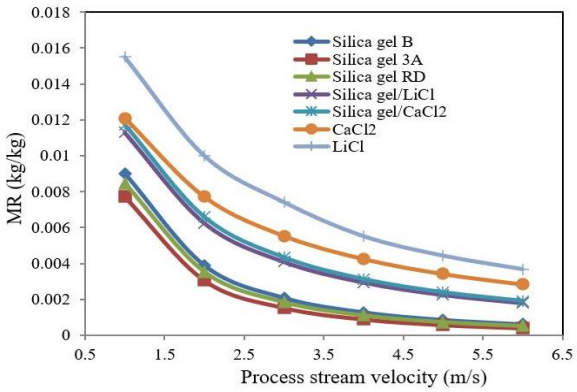

Fig. 11: Graph of MR with process stream velocity for different desiccant wheels

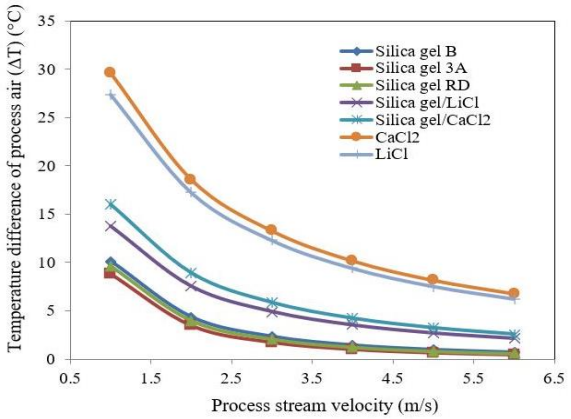

Fig. 12: Graph of temperature difference with process stream velocity for different desiccants wheels

Fig. 12 shows that there is a greater impact of process velocity on a ΔT of process air, especially for group 2 and 3 wheels. Here the maximum ΔT for process air of group 2 wheels is very high i.e. 25 to 30℃. This is only because of higher heat of adsorption and more contact (residence) time of air in the sinusoidal channel, as regeneration temperature is already fixed in the lower side i.e. 60℃. For group 1 and group 3 wheels, this temperature difference is 10 to 15 ℃, respectively. However, in all the above cases the temperature difference is less than 10 ℃ for all wheels because process velocity is fixed on the higher side i.e. 4 m/s. Therefore, we can choose group 3 as a better desiccant wheel since, in the higher process velocities, the temperature difference is less than 5℃ and MR is also higher than group 1. But higher process velocity also increases the fan power. Hence, the optimum process stream velocity should be in the range of 2 to 3 m/s.

4.1.5 Analysis of the MR and ΔT of process air at a different process inlet temperature

As we know, the rise in process air inlet temperature reduces MR since the difference of vapour pressure in the moisture transfer zone decreases with an increase in temperature. Fig. 13 shows that the influence of process inlet temperature on group 2 and group 3 wheels is

higher than on group 1. The MR of group 1 and 3 wheels becomes very low when we increase the beyond 40℃. Therefore, in the higher range of process inlet temperature, i.e. above 40℃, group 2 materials are better desiccants.

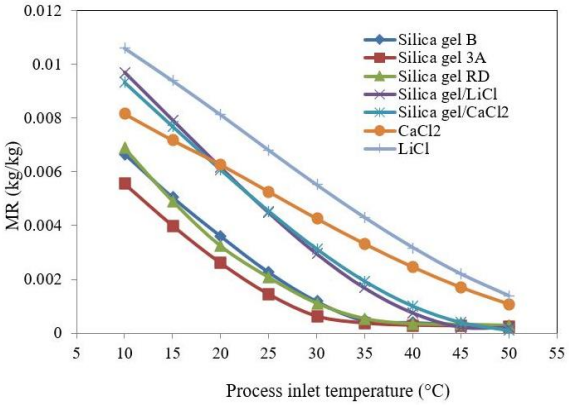

Fig. 13: Graph of MR with process inlet temperature for different desiccant wheels

Fig. 14 shows the effect of process inlet temperature on theΔT for different desiccants, and it has been found that the temperature difference is higher for group 2 wheels due to the larger heat of adsorption. Also, the effect of process inlet temperature on group 2 is higher than in groups 1 and 3. In between 10 to 35℃, group 3 material can be considered as a better desiccant due to moderate MR and less ΔT , while in the higher temperatures, group 2 materials can be considered as better desiccants because, in this range, group 2 have higher MR than the group 1 and 3. At this condition increase in $\Delta T$for group 2 is less than 6℃, which is considerable because this value is comparatively less than from all the above cases.

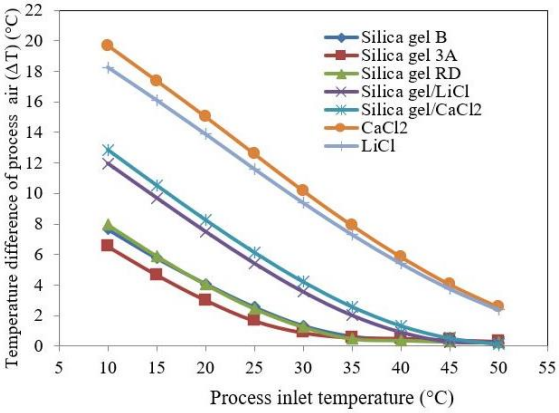

Fig. 14: Graph of temperature difference with process inlet temperature for different desiccant wheels

4.1.6 Analysis of MR and ΔT of process air at different process inlet humidity ratio

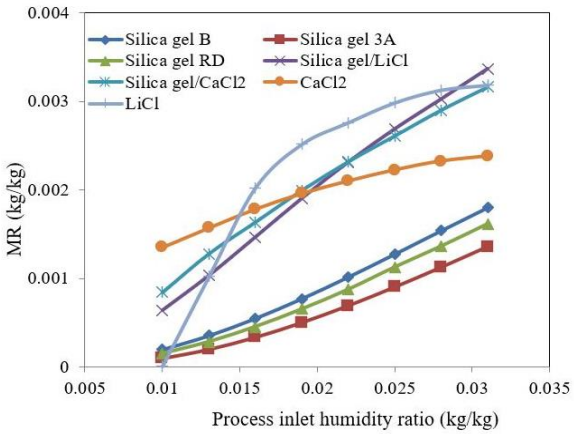

Fig. 15: Graph of MR with process inlet humidity ratio for different desiccant wheels

Fig. 15 shows that MR rises with a rise in process inlet humidity ratio for all desiccants. Specifically, the MR of group 2 material start flattening with the increase in humidity, but this does not happen for group 1 and 3. Because group 2 has a higher heat of sorption, consequently vapour pressure difference between air streams and desiccant walls decreases, and the curve starts flattening. At low humidity and very high humidity, group 2 and 3 material has higher MR than group 1 material. But between 0.015 to 0.025 $kg\,kg^{-1}$, LiCl of group 2 has maximum MR. The MR of LiCl varies from very low value to very high value (0.0031827310 $kg\,kg^{-1}$) when the process inlet humidity ratio varies from 0.01 to 0.035$kg\,kg^{-1}$. Therefore, we can conclude that the process inlet humidity ratio has a greater impact on the MR of LiCl than the other desiccants.

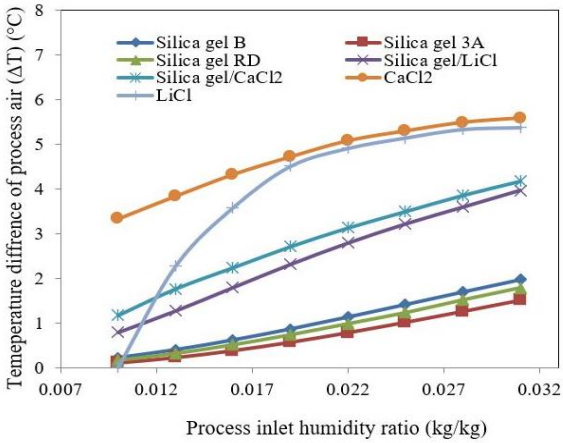

Fig. 16: Graph of temperature difference with process inlet humidity ratio for different desiccant wheels

Fig. 16 shows the influence of inlet humidity on temperature difference(ΔT) of process air where we can observe that the maximum temperature difference occurs for CaCl2 material however the maximum moisture removal occurs for LiCl desiccants. The influence of process inlet humidity ratio on a temperature difference(ΔT) of process air is similar to the above case.

As per Fig. 16, LiCl cannot be considered a better desiccant because its ΔT is also higher, which is not desirable in the DWBACS system. Further, in the higher RH environment, LiCl may mix with air, and that may cause the loss of desiccant coating. Therefore, in this case, also group 3 materials can be considered as a superior desiccant due to higher MR and moderate ΔT.

5. Conclusions

In this study, the influence of different desiccant wheels has been investigated at altered operating conditions by solving a one-dimensional mathematical model with the help of FlexPDE. The following conclusion is made from the comparison of different desiccant wheels.

1. Group 2 desiccant wheels have considerably higher ΔT than the other wheels. The maximum value even reaches up to 30℃. Hence, group 2 wheels cannot be recommended for air conditioning applications.
2. In terms of energy consumption and MR also, group 3 wheels and LiCl wheel performs better than the other wheels. Because, in lower regeneration temperatures (50 to 70℃) and lower regeneration velocities (1 to 2 m/s), the MR of group 3 wheels is higher than the other wheels. But ΔT obtained from the LiCl wheel is also higher. Since the lower regeneration temperature and lower regeneration velocities are the assessment of lesser energy consumptions. Hence, group 3 wheels can be recommended for air conditioning based on energy consumption also.
3. In the case of higher ranges of process inlet temperature (40 to 50℃), MR obtained from group 2 wheels is higher than the other wheels and also obtains approximately similar ΔT. But in lower ranges of process inlet temperature (10 to 20℃), group 3 wheels give higher MR with moderate ΔT.
4. In the areas of very low humidity (0.05 to 0.013 kg/kg) and high humidity (beyond 0.02 k/kg at 30℃) also, group 3 wheels perform (higher MR and moderateΔT) better than the other desiccant wheels

6. Future work scope

In future, research can be done on use of desiccant material on different operating conditions like Hot and humid, Hot and dry, Cool and humid, Cool and dry.

Nomenclature

a	channel height (mm)
A_{csdl}	cross-sectional area of the desiccant layer
A_{csf}	cross sectional area of flow passage of one channel (m^2)
b	pitch of the channel (mm)
c_p	specific heat at constant pressure ($J.kg^{-1}.K^{-1}$)
c_{pw}	specific heat of liquid water ($J.kg^{-1}.K^{-1}$)
c_{pm}	specific heat of substrate (matrix material) ($J.kg^{-1}.K^{-1}$)
D	diameter of desiccant wheel (m)
D_{hf}	Hydraulic diameter of channel (m)
D_m	mass diffusion coefficient of water vapour in the air (-)
h_{fg}	latent heat of vapourization ($J.kg^{-1}$)
h_m	mass transfer coefficient ($kg.m^{-2}.s^{-1}$)
H	convective heat transfer coefficient (W/m^2K)
K	Thermal conductivity ($W.m^{-1}.K^{-1}$)
L	Wheel Length (m)
P_f	Perimeter of a flow passage (m)
W_{max}	maximum water content in desiccant ($kg_{adsorbate}\ kg_{adsorbent}^{-1}$)
x	axial direction
Y	humidity ratio of the air ($kg\ kg^{-1}$)

Greek symbols

ρ	density ($kg.m^{-3}$)
ϵ	porosity (-)
θ	fraction angle (Degree)
δ_d	channel wall thickness (mm)
φ	volume ratio (-)

Subscripts

a	air
atm	atmospheric
d	desiccant
ad	adsorbent
da	dry air
f	flow passage
m	matrix material
p	process air
r	regeneration air
v	vapour
0	initial state

Abbreviations

DW	Desiccant wheel
DCOP	dehumidification coefficient of performance
DWBACS	desiccant wheel-based air conditioning system
EXP	experimental
MATH	mathematical
PDE	partial differential equation
RS	regeneration sector
SDP	specific dehumidification power
SIM	simulation
PS	process sector

Conflict of interest: On behalf of the authors, the corresponding author states that there is no conflict of interest.

References

1) S. Farooq, and D.M. Ruthven, "Numerical simulation of a desiccant bed for solar air conditioning applications," *J. Sol. Energy Eng. Trans. ASME*, **113** (*2*) 80–88 (1991). doi:10.1115/1.2929962.
2) G. Singh, "A novel design of triple-hybrid absorption radiant building cooling system with desiccant dehumidification," **141** (*July*) 1–13 (2019). doi:10.1115/1.4042239.
3) G. Singh, and R. Das, "A novel variable refrigerant flow system with solar regeneration-based desiccant-assisted ventilation," *Sol. Energy*, **238** (*March*) 84–104 (2022). doi:10.1016/j.solener.2022.04.008.
4) A. Fauzan, H.M. Ega, J.A. Sigalingging, and Y.S. Nugroho, "Analysis of heat gains from flat plate heater measured using multi-axis heat flux sensors," *Evergreen*, **8** (*4*) 844–849 (2021). doi:10.5109/4742130.
5) A. Dhiman, and G. Sachdeva, "Energy and exergy analysis of a pressurized solar cooking system based on a parabolic dish collector," *Evergreen*, **9** (*4*) 1168–1180 (2022). doi:10.5109/6625728.
6) R. Narayanan, W.Y. Saman, and S.D. White, "A non-adiabatic desiccant wheel: modeling and experimental validation," *Appl. Therm. Eng.*, **61** (*2*) 178–185 (2013). doi:10.1016/j.applthermaleng.2013.07.007.
7) M.J. Goldsworthy, and S. White, "Design and performance of an internal heat exchange desiccant wheel," *Int. J. Refrig.*, **39** 152–159 (2014). doi:10.1016/j.ijrefrig.2013.10.009.
8) A.K. Verma, L. Yadav, N. Kumar, and A. Yadav, "Mathematical investigation of different parameters of the passive desiccant wheel," *Numer. Heat Transf. Part A Appl.*, 1–20 (2023). doi:10.1080/10407782.2023.2172491.
9) C.P. Arora, "Refrigeration and air conditioning," 3rd ed., 2016.
10) T.K. BB Saha, EC Boelman, "Computational analysis of an advanced adsorption-refrigeration cycle," *Energy*, **20** (*10*) 983–994 (1995).
11) A. Yadav, "Experimental and Numerical Investigation of Solar Powered Solid Desiccant Dehumidifier," NIT Kurukshetra, 2012.
12) J. Miyawaki, J. Yeh, H.S. Kil, J.K. Lee, K. Nakabayashi, I. Mochida, and S.H. Yoon, "Influence of pore size and surface functionality of activated carbons on adsorption behaviors of indole and amylase," *Evergreen*, **3** (*2*) 17–24 (2016). doi:10.5109/1800868.
13) Pahwa D., Choudhary, A. K., "(12) patent application publication (10) pub . no .: us 2016 / 0271610 a1 patent application publication," **1** (*19*) 1–5 (2016).
14) A.K. Prasad, "Comparative analysis of different design of rotary dehumidifier," *Heat Transf. Res.*, (*January*) 193–215 (2019). doi:10.1002/htj.21480.
15) A. Yadav, L. and Yadav, "Parametric analysis of desiccant wheel for air conditioning application," *Heat Transf. - Asian Res. Res.*, (*May*) 1–23 (2018). doi:10.1002/htj.21338.
16) T.S. Ge, F. Ziegler, and R.Z. Wang, "A mathematical model for predicting the performance of a compound desiccant wheel (a model of compound desiccant wheel)," *Appl. Therm. Eng.*, **30** (*8–9*) 1005–1015 (2010). doi:10.1016/j.applthermaleng.2010.01.012.
17) G. Angrisani, A. Capozzoli, F. Minichiello, C. Roselli, and M. Sasso, "Desiccant wheel regenerated by thermal energy from a microcogenerator: experimental assessment of the performances," *Appl. Energy*, **88** (*4*) 1354–1365 (2011). doi:10.1016/j.apenergy.2010.09.025.
18) L. Yadav, and A. Yadav, "Effect of different arrangements of sector on the performance of desiccant wheel," *Heat Mass Transf. Und Stoffuebertragung*, **54** (*1*) 7–23 (2018). doi:10.1007/s00231-017-2092-6.
19) X. Zheng, T.S. Ge, and R.Z. Wang, "Recent progress on desiccant materials for solid desiccant cooling systems," *Energy*, **74** (*1*) 280–294 (2014). doi:10.1016/j.energy.2014.07.027.
20) T.S. Ge, Y.J. Dai, R.Z. Wang, and Y. Li, "Performance of two-stage rotary desiccant cooling system with different regeneration temperatures," *Energy*, **80** 556–566 (2015). doi:10.1016/j.energy.2014.12.010.
21) S.D. White, M. Goldsworthy, R. Reece, T. Spillmann, A. Gorur, and D.Y. Lee, "Characterization of desiccant wheels with alternative materials at low regeneration temperatures," *Int. J. Refrig.*, **34** (*8*) 1786–1791 (2011). doi:10.1016/j.ijrefrig.2011.06.012.
22) M.H. Mahmood, M. Sultan, and T. Miyazaki, "Study on water-vapor adsorption onto polymer and carbon based adsorbents for air-conditioning applications," *Evergreen*, **6** (*3*) 215–224 (2019). doi:10.5109/2349297.
23) M.N. Golubovic, H.D.M. Hettiarachchi, and W.M. Worek, "Evaluation of rotary dehumidifier performance with and without heated purge," *Int. Commun. Heat Mass Transf.*, **34** (*7*) 785–795 (2007). doi:10.1016/j.icheatmasstransfer.2007.03.011.

24) L. Yadav, and A. Yadav, "Mathematical investigation of purge sector angle for clockwise and anticlockwise rotation of desiccant wheel," *Appl. Therm. Eng.*, **93** 839–848 (2016). doi:10.1016/j.applthermaleng.2015.10.062.
25) M.A. Mandegari, S. Farzad, G. Angrisani, and H. Pahlavanzadeh, "Study of purge angle effects on the desiccant wheel performance," *Energy Convers. Manag.*, **137** 12–20 (2017). doi:10.1016/j.enconman.2017.01.042.
26) R. Narayanan, W.Y. Saman, S.D. White, and M. Goldsworthy, "Comparative study of different desiccant wheel designs," *Appl. Therm. Eng.*, **31** (*10*) 1613–1620 (2011). doi:10.1016/j.applthermaleng.2011.01.043.
27) P. Majumdar, "HEAT and mass transfer in composite desiccant pore structures for dehumidification," *Sol. Energy*, **62** (*1*) 1–10 (1998).
28) X.J. Zhang, K. Sumathy, Y.J. Dai, and R.Z. Wang, "Dynamic hygroscopic effect of the composite material used in desiccant rotary wheel," *Sol. Energy*, **80** 1058–1061 (2006). doi:10.1016/j.solener.2005.07.008.
29) A. Al-Alili, Y. Hwang, and R. Radermacher, "Performance of a desiccant wheel cycle utilizing new zeolite material: experimental investigation," *Energy*, **81** 137–145 (2015). doi:10.1016/j.energy.2014.11.084.
30) M. Intini, M. Goldsworthy, S. White, and C.M. Joppolo, "Experimental analysis and numerical modelling of an aqsoa zeolite desiccant wheel," *Appl. Therm. Eng.*, **80** 20–30 (2015). doi:10.1016/j.applthermaleng.2015.01.036.
31) L.Z. Zhang, H.X. Fu, Q.R. Yang, and J.C. Xu, "Performance comparisons of honeycomb-type adsorbent beds (wheels) for air dehumidification with various desiccant wall materials," *Energ1) L.Z. Zhang, H.X. Fu, Q.R. Yang, J.C. Xu, "Performance Comp. Honeycomb-Type Adsorbent Beds Air Dehumidification with Var. Desiccant Wall Mater. Energy, 65 430–440 (2014). Doi10.1016/j.Energy.2013.11.042.Y*, **65** 430–440 (2014). doi:10.1016/j.energy.2013.11.042.
32) L.A. Sphaier, and W.M. Worek, "Comparisons between 2-d and 1-d formulations of heat and mass transfer in rotary regenerators," *Numer. Heat Transf. Part B Fundam.*, **49** (*3*) 223–237 (2006). doi:10.1080/10407790500434166.
33) X.J. Zhang, Y.J. Dai, and R.Z. Wang, "A simulation study of heat and mass transfer in a honeycombed rotary desiccant dehumidifier," *Appl. Therm. Eng.*, **23** 989–1003 (2003). doi:10.1016/S1359-4311(03)00047-4.
34) J.D. Chung, and D.Y. Lee, "Effect of desiccant isotherm on the performance of desiccant wheel," *Int. J. Refrig.*, **32** (*4*) 720–726 (2009). doi:10.1016/j.ijrefrig.2009.01.003.
35) A. Kodama, "Experimental study on optimization of a honeycomb rotor continuous adsorber operated with thermal swing," Kumamoto University Japan, 1995.
36) U. Eicker, U. Schürger, M. Köhler, T. Ge, Y. Dai, H. Li, and R. Wang, "Experimental investigations on desiccant wheels," *Appl. Therm. Eng.*, **42** 71–80 (2012). doi:10.1016/j.applthermaleng.2012.03.005.